AGU ADVANCING EARTH AND SPACE SCIENCE

Water Resources Research

RESEARCH ARTICLE
10.1029/2020WR029049

Tracing and Closing the Water Balance in a Vegetated Lysimeter

Paolo Benettin[1], Magali F. Nehemy[2], Mitra Asadollahi[1], Dyan Pratt[2], Michaël Bensimon[3], Jeffrey J. McDonnell[2,4], and Andrea Rinaldo[1,5]

[1]Laboratory of Ecohydrology ENAC/IIE/ECHO, École Polytechinque Fédérale de Lausanne (EPFL), Lausanne, Switzerland, [2]Global Institute for Water Security, School of Environment and Sustainability, University of Saskatchewan, Saskatoon, SK, Canada, [3]Central Environmental Laboratory ENAC/IIE/CEL, École Polytechinque Fédérale de Lausanne (EPFL), Lausanne, Switzerland, [4]School of Geography, Earth and Environmental Sciences, University of Birmingham, Birmingham, UK, [5]Dipartimento ICEA, Università degli studi di Padova, Padua, Italy

Key Points:

- Labeled tracer experiment on a large vegetated soil column
- Tracing precipitation through the entire soil water balance
- Travel time to transpiration very different from travel time to bottom drainage

Supporting Information:

Supporting Information may be found in the online version of this article.

Correspondence to:

P. Benettin,
paolo.benettin@epfl.ch

Citation:

Benettin, P., Nehemy, M. F., Asadollahi, M., Pratt, D., Bensimon, M., McDonnell, J. J., & Rinaldo, A. (2021). Tracing and closing the water balance in a vegetated lysimeter. *Water Resources Research*, *57*, e2020WR029049. https://doi.org/10.1029/2020WR029049

Received 15 OCT 2020
Accepted 17 MAR 2021

Abstract Closure of the soil water balance is fundamental to ecohydrology. But closing the soil water balance with hydrometric information offers no insight into the age distribution of water transiting the soil column via deep drainage or the combination of soil evaporation and transpiration. This is a major challenge in our discipline currently; tracing the water balance is the needed next step. Here we report results from a controlled tracer experiment aimed at both closing the soil water balance and tracing its individual components. This was carried out on a 2.5 m^3 lysimeter planted with a willow tree. We applied 25 mm of isotopically enriched water on top of the lysimeter and tracked it for 43 days through the soil water, the bottom drainage, and the plant xylem. We then destructively sampled the system to quantify the remaining isotope mass. More than 900 water samples were collected for stable isotope analysis to trace the labeled irrigation. We then used these data to quantify when and where the labeled irrigation became the source of plant uptake or deep percolation. Evapotranspiration dominated the water balance outflow (88%). Tracing the transpiration flux showed further that transpiration was soil water that had fallen as precipitation 1–2 months prior. The tracer breakthrough in transpiration was complex and different from the breakthrough curves observed within the soil or in the bottom drainage. Given the lack of direct experimental data on travel time to transpiration, these results provide a first balance closure where all the relevant outflows are traced.

1. Introduction

The water balance is ecohydrology's most important equation. Rodriguez-Iturbe (2000) notes that although apparently simple, it still presents serious challenges when infiltration, evapotranspiration, and leakage are all dependent on soil moisture dynamics. While useful, the black box water accounting model is unable to mechanistically assess mixing dynamics, ages of the water fluxes, and partitioning dynamics. Because of this, there have been recent calls for a different way of addressing the water balance (McDonnell, 2017)–one that tracks both the input-storage-output relations and the age of each component. This is because closure of the water balance (annually, the tradition in catchment hydrology) is physically unrealistic when individual water balance components can greatly exceed 1 year. Indeed, traditional hydrometric approaches to water balance closure only describe *how much* water flows through a system and not *which* water.

In a recent review, Sprenger et al. (2019) noted that empirical water age data in the critical zone remains scarce and "with improving technology, we are gaining insights into the diversity of water ages within pools that have been elsewhere treated as well-mixed buckets." Some examples include the fact that two third of groundwater below 250 m is more than 10,000 years old (Jasechko et al., 2017); that often summer transpiration can be older water from previous seasons (Allen et al., 2019; Brooks et al., 2010). In extreme cases transpired water can be many months or years old (Zhang et al., 2017); Generally, stored water is much older than the stream waters that drain them (Berghuijs & Kirchner, 2017)–with stream waters themselves often in the years to decades age range (McGuire & McDonnell, 2006).

But while tracer data in streamflow is now relatively abundant (Penna et al., 2018; Sprenger et al., 2019) and available at high resolution (Rode et al., 2016; von Freyberg et al., 2017), a major share of the water balance still goes through an outlet that is almost unmonitored in terms of tracers: the transpiration flux.

Thus, the quantitative determination of *which* age of water is used by plants remains a challenge. And this is a Lagrangian problem–one that deals with the need to compute the trajectory of individual water parcels.

The combined use of transport models (e.g. Ala-aho et al., 2017; Asadollahi et al., 2020; Kuppel et al., 2018; Maxwell et al., 2018; Pangle et al., 2017; Sprenger et al., 2018; Wilusz et al., 2017; Yang et al., 2018) and the collection of tracer data from xylem samples (e.g. Allen et al., 2019; Beyer et al., 2020; Penna et al., 2018; Volkmann et al., 2016) can help tackle this problem. However, two barriers exist: 1) transport models need to make significant assumptions about the way vegetation takes up water of different depths, ages, or held in different pore spaces, and few data enable such model testing; and 2) most experimental evidence on plant uptake is based on snapshot measurements of environmental tracers, and we fundamentally lack high-resolution tracer breakthrough curves for the transpiration flux. So are we able to trace the age of the transpiration flux and when an individual rainfall event is taken up by plants following infiltration? In other words, can we trace and close the Lagrangian mass balance experimentally, for one or more labeled precipitation events?

In open environmental systems, tracing the water balance is extraordinarily difficult due to often unknown boundary conditions (see von Freyberg et al., 2020). One intermediate step toward this goal is with controlled laboratory experiments and lysimeters, where boundary conditions can be controlled or measured. Here, we implement some of the recommendations in Sprenger et al. (2019), who advocated "to further develop sampling designs and new measurement techniques" and "better understanding of where, when, and how often to take samples in tracer hydrological investigations" for improving our understanding of the demographics of water in the critical zone. We also build on calls by Soulsby et al. (2016) for characterizing the age distribution of catchment evaporative losses, something largely still beyond our reach in the field. We do this by working with a vegetated lysimeter and a combined hydrometric monitoring of all water balance components and a labeled 43 days tracer experiment.

Here we determine experimentally the tracer breakthrough curve in the transpiration flux for a 2.5 m^3 vegetated lysimeter located within the EPFL campus (CH). We build on the previous experiments by Queloz et al. (2015), Benettin et al. (2019) and here apply 25 mm of isotopically enriched water on the upper surface of the lysimeter and track it for 43 days through the soil water, the bottom drainage, and the plant xylem for a 6-year-old willow tree (*Salix viminalis*) growing within the lysimeter. Our goal is to track experimentally the labeled precipitation through the entire water balance defined by the known lysimeter volume. We test the hypothesis that high-resolution measurements of water fluxes and tracer concentration allow for the experimental closure of the lysimeter tracer balance with explicit accounting of residual measurement uncertainty. Our main research questions are thus: 1) can we close the lysimeter water balance experimentally? 2) How does a tracer-based closure compare to a hydrometry-based closure? 3) What is the residence time of transpiration compared to soil water and bottom drainage residence times? Finally, we take soil cores following the 43 days experiment to attempt to quantify the remaining isotope mass in the system and trace and seek closure to the Lagrangian mass balance.

2. Methods

2.1. Experimental Design

The "Spike II" experiment was designed to achieve the experimental tracer balance closure in a large vegetated lysimeter located within the EPFL campus in Lausanne (CH). The experiment consisted in the application of an isotopically labeled irrigation ("spike" irrigation) and its tracking within the soil column and in all outflows including, critically, vegetation.

The lysimeter (Figure 1) is a 2.5 m-deep and 1.12 m^2-surface fiberglass column that was previously used to investigate the transport of fluorobenzoids and isotope tracers through soil (Benettin et al., 2019; Queloz et al., 2015). The main experimental setup is the same as Queloz et al. (2015): the lysimeter was filled in 2012 with sandy soil (approximately 50% loamy sand from a nearby construction site and 50% lacustrine sand from lake Geneva) which was not meant to be representative of any soil in particular. Right after filling, two small, genetically identical willow trees (*Salix viminalis*) were planted. The plants were cut at the base in 2014 but re-grew until the beginning of the experiment (May 2018). The column is easily accessible through an underground chamber. The bottom of the column hosts a 50 cm gravel filter to facilitate drainage and it is

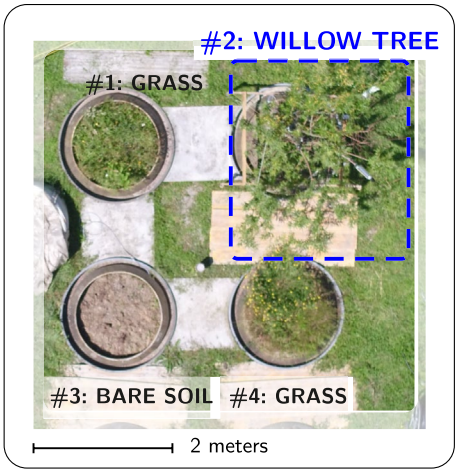

SAMPLES for ISOTOPE ANALYSIS

sample type	*frequency*	*n*
bottom drainage	all events	37
bulk soil water	4 days	130
suction cups (-0.6 bar)	2 days	318
xylem	max 4 days	59
phloem	irregular	34
leaves	irregular	26
precipitation	all events	22
irrigation (tap water)	all events	10
atmospheric vapor	irregular	8
bulk soil profiles	begin and end	76

MEASUREMENTS

Bottom drainage flow	Vol. Water Content
Precipitation flow	sap flow (3 branches)
Irrigation flow	dendrometer (3 branches)
ET flow (from weight)	leaf area
Soil Temperature	root density and depth
Soil tension	branch architecture

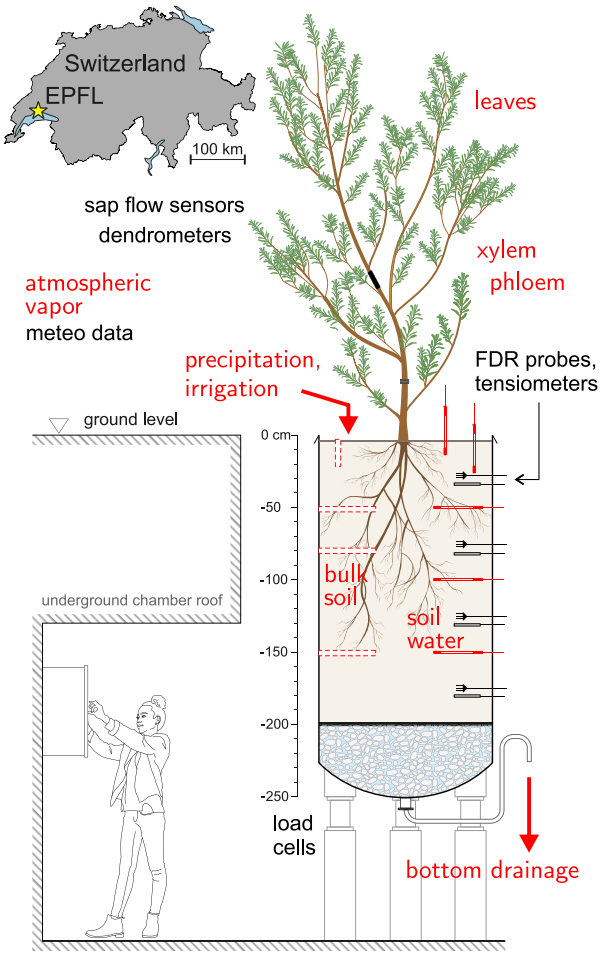

Figure 1. Sketch of the experimental setup. The tracer addition consisted in 25 mm of water highly enriched in both $\delta^{18}O$ (+29.6‰) and $\delta^{2}H$ (+256.6‰). The tracer was tracked for 43 days within the soil column, in the bottom flow, and in the plant. Red color denotes water compartments that were sampled for isotopic analyses.

separated from the soil through a geotextile. A syphon was used to avoid the water table from falling below the depth of 210 cm and to achieve a realistic pressure profile within the column (Queloz et al., 2015). No water was added from below to keep the water table at a fixed depth. The gravel filter is expected to have little impact on tracer transport because the water storage in the filter is less than 30 L compared to a total water storage in the lysimeter varying between 300 and 500 L.

In the two years before the beginning of the experiment, the lysimeter was let open to natural precipitation and was sometimes irrigated with tap water to avoid water stress. The labeled irrigation consisted in 25 mm of water, which is a volume consistent with summer storms in the area, and it was isotopically highly enriched in both $\delta^{18}O$ (+29.6‰) and $\delta^{2}H$ (+256.6‰). Such a composition was designed by mixing the local tap water ($\delta^{18}O = -12.3$‰, $\delta^{2}H = -90.4$‰) with deuterium oxide ($^{2}H_2O$; 99.5% Cambridge Isotopes, Cambridge, MA, USA) and oxygen-18 water ($H_2^{18}O$; 97.7% Medical Isotopes, Pelham, NH, USA). The isotope values of the labeled irrigation are significantly higher than typical local precipitation (whose mean monthly values range in (−12, −5)‰ $\delta^{18}O$ and (−85, −35)‰ $\delta^{2}H$) and they approximately lie on the same local meteoric water line (LMWL). The irrigation was applied through a drop sprinkler over 2 h on the evening of 16 May 2018. After application, the tracer was tracked through the system until 29 June 2018 (43 days) before the experiment was stopped and the soil column and the plant destructively sampled. During the experiment, the lysimeter was let open to natural precipitation and additional irrigation was applied to achieve dry-wet-dry cycles. The reason for an experiment duration of 6 weeks was the need to balance the high resolution and the damage to the willows due to the removal of stems for xylem sampling. Specific

details of this experiment concerning the tree water deficit dynamics and the isotope composition of leaf water are described by Nehemy et al. (2021) and Benettin et al. (2021).

A meteo station (MeteoMADD, MADD Technologies Sàrl, Switzerland) located 5 m from the lysimeter provided meteorologic data (precipitation through a tipping bucket, air temperature, solar radiation, humidity, wind speed). Drainage from the lysimeter base was measured through a tipping bucket (Casella Measurement, UK, reported accuracy: ±2% at 1 mm/h) and flow was averaged over 15 min intervals. Evapotranspiration was computed from the measured weight variations (see Section 2.3). Irrigation was always supplied at night, when evapotranspiration was minimal and computed through the measured (positive) weight variations. Three other weighed lysimeters of the same type (one with bare soil and two covered with grass) were in function during the experiment and they were used to measure precipitation and to have a qualitative comparison of ET dynamics in similar lysimeters with different covers. An evaporation pan (1.12 m^2 by 0.2 m) was also put in place to determine evaporation from an open water surface. All data were aggregated at 15 min resolution. Volumetric water content and temperature within the soil column were measured through a total of eight frequency domain reflectometry (5 TM Devices Inc., USA) probes installed at depth of 25, 75, 125 and 175 cm (2 probes per depth). Soil tensiometers (TensioMark; ecoTech UmweltMeβsysteme GmbH, Germany) were also installed at the same depths (1 per depth). The willow trees had three main stems with an average diameter of 29 mm at 50 cm above the ground. Each stem was instrumented with a dendrometer (Ecomatik, Germany; small diameter dendrometers DD-S, accuracy ±1.5 μm) to monitor stem radius change and a sap flow sensor (EXO-Skin SGA19; SGA 25, SGA 25 Dynamax, Houston, TX, USA). Sap flow sensors were installed just above the dendrometers, and one of the main stems had a second sap flow sensor installed closer to the crown. As sap flow sensors had to be installed above some lateral branches, they only provided a qualitative measure of transpiration dynamics and could not be used to quantify the magnitude of the transpiration flux. We also monitored leaf water potential at crown with the use of a leaf psychrometer (PSY 1, ICT International, Australia). All the tree instruments provided 15 min resolution data. Tree height was approximately 3 m with a crown area of about 4 m^2. The root system was 2 m deep in the lysimeter. The willows showed a relatively high fine root (<2 mm) length density (RLD) and root tissue density. Specifically, RLD was found to be higher at shallow layers (14.24 cm cm^{-3}) with smaller, but still present fine roots in the bottom of the lysimeter (6.47 cm cm^{-3}) (Nehemy et al., 2021).

2.2. Sample Collection and Analysis

We sampled xylem, phloem, and leaves from the tree; bulk soil and soil water; precipitation, irrigation, and bottom drainage. All these samples were analyzed for their isotope composition. We collected soil for posterior water extraction at five different depths: 10, 25, 50, 80, and 150 cm, with three replicates per depth, every four days. The depth of 100 cm was not technically possible to sample because of the configuration of the lysimeter chamber. We sampled soil using an auger with 3 cm in diameter and horizontally coring the soil column through small ports, proceeding toward the center of the lysimeter. We used the same ports every time of sampling. We collected approximately 8 cm of soil with the auger and discarded the outermost 3 cm. After sampling, we filled the access port and empty space with a PVC pipe of similar diameter and rubber band to minimize preferential flow paths, and condensation in the orifice. The first two depths (10 and 25) were collected using the same auger, but vertically from the soil surface, and alternating sampling location. We immediately stored soil samples in 12 ml Exetainer vials (Labco Ltd, UK). On 29 June, we collected three soil cores at 10 cm resolution to improve spatial representation of soil isotopic composition at the end of the experiment.

Tree samples were collected at higher-temporal frequency in the beginning of the experiment. We collected xylem on a daily basis during the first 11 days after tracer injection. This was possible because of willow's crown architecture with vast amount of long and suberized branches. After this periods, we decreased the sampling frequency to every other day, until 10 June. We, then, decreased to same frequency as bulk soil water until 22 June, and returned to a daily basis until the end of the experiment on 29 June. Although the willow had numerous branches, we decreased sampling frequency in the middle of the experiment to avoid reducing significantly tree crown area, while allowing higher-frequency sampling during specific intervals to capture the dynamics of the transpiration process. There were four days when we collected samples throughout the transpiration diurnal cycle (predawn, midday, afternoon, and night) obtaining higher

frequency measurements. After 30 May, samples of phloem and leaves were collected from the same branch as the xylem.

We collected plant material only from well-developed and suberized branches. We recorded branch length and diameter and location in relation to the three main stems. Besides the samples collected under 24 h periods, we sampled at midday when transpiration is at peak. After removing branch from the tree, we immediately covered the wound with silicone to minimize any evaporation from exposed surface. The sampled branch was quickly processed, separating the phloem and xylem and storing them in separated vials, as well as leaves. All tree material was immediately stored in 12 ml Exetainer vials used later for cryogenic extraction.

2.2.1. Samples Directly Available for Isotope Analyses

The samples that did not need posterior water extraction, such as soil water, precipitation, irrigation, and bottom drainage were sampled, filtered through a 0.45 μm filters, and stored in 2 mL vials with septum screw caps (2 mL Clear Vial, Canadian Life Science, Canada). Soil water samples were collected at depths of 10, 25, 50, 100, and 150 cm, with three spatially distributed sampling points per depth. We used an automated suction system that worked at −0.6 bar and directly extracted the water from the soil. We also collected sporadically soil water samples from the soil surface of the grass-planted lysimeter. We used a precipitation collector installed 2 m away from the lysimeter to sample rainfall events. We also occasionally collected atmospheric vapor through vacuum bottles. Additionally, water samples were collected from an evaporation pan located 10 m away from the lysimeter. All water, soil, and tree samples were stored at 4 °C until analysis.

The isotopic content of water samples were determined independently at two laboratories: the CEL laboratory at EPFL, through a Cavity Ring Down Spectrometer L2130-*i* (Picarro, United States), and at the Hillslope Hydrology laboratory at University of Saskatchewan through a IWA-45EP off-axis integrated cavity output spectroscopy (OA-ICOS) (Los Gatos Research Inc., United States). Laboratory precision was ±1.0‰ and ±0.2‰ for δ^2H and δ^{18}O, respectively.

2.2.2. Samples That Needed Water Extraction Prior to Isotope Analyses

We extracted the water from bulk soil and tree samples and conducted posterior isotopic analysis at the Hillslope Hydrology Laboratory. We used a cryogenic vacuum distillation system detailed by Koeniger et al. (2011) to extract water from soil xylem, phloem, or leaves. 12 ml Exetainer vials contained approximately 2 g of plant material, and 10 g of soil per vial, prior water extraction. Vials were weighted before and after cryogenic extraction to ensure extraction efficiency above 98%. After extraction, plant and soil water samples were filtered through a 0.45 μm filters, and stored in 2 mL vials with septum screw caps for isotopic analysis. We analyzed the isotopic composition of bulk soil water on OA-ICOS, and xylem, phloem, and leaves using isotope ratio mass spectrometry (IRMS) to avoid spectral contamination.

2.3. Data Processing

2.3.1. Computing ET and Precipitation From Weight Data

Timeseries of ET from all four lysimeters (i.e., one with the willow trees, two covered in grass, and one bare soil) were determined from the measured weight variations. The weight signal was acquired at 20 s resolution and then filtered to remove large outliers and occasional disturbances (see Schrader et al., 2013). ET was then computed by solving the continuity equation under the assumption that precipitation $P(t)$, irrigation $Ir(t)$ (that always took place at night-time), and evapotranspiration $ET(t)$ did not occur simultaneously:

$$P(t) + Ir(t) - ET(t) = \frac{dW(t)}{dt} + L(t) \quad (1)$$

where t is time, W is the recorded weight (kg) divided by the lysimeter surface and $L(t)$ is the measured bottom leakage flux. Equation 1 was solved at 15 min resolution and the resulting precipitation was compared across lysimeters and with data from the meteo station to ensure consistency. ET was further smoothed to reduce noise during windy days (see also Groh et al., 2018; Hannes et al., 2015; Peters et al., 2017). We applied a low-pass filter with passband frequency of 24 h and stopband frequency of 4 h, which is ultimately

similar to a moving average filter with window of 3 h without delay. Measurements for the bare soil lysimeter only started after 4 June (i.e., 18 days after the experiment start) and therefore no ET was computed for this lysimeter before that date. Occasional data gaps were filled through a linear regression with sap flow measurements (for the willow-planted lysimeter) or with the Penman-Monteith model (for the other lysimeters). The difference between ET from the bare soil lysimeter and the willow-planted lysimeter, together with isotope methods (see Section 2.3.2) was used to estimate the partitioning of ET into evaporation and transpiration for the willow-planted lysimeter (Section 3.3).

2.3.2. Accounting for Isotope Evaporative Fractionation

The isotopic enrichment due to isotope fractionation can be problematic when one wants to retrieve the breakthrough curve of a labeled precipitation (see Benettin et al., 2019) because it causes an enrichment of heavy water molecules in the liquid phase compared to the most abundant water molecules. Moreover, the two stable isotopes have different degrees of fractionation and result in inconsistent breakthroughs. Evaporative fractionation can be interpreted as a special case of reactive transport that causes the tracer to be non-conservative. To retrieve the breakthrough curves of water itself, it is thus necessary to account for the effect of isotopic fractionation. We use the method by Bowen et al. (2018) to estimate the composition of the source water before it became fractionated and thus we reconstruct the tracer breakthrough that would have been observed had the tracer been fully conservative. An example of the effect of fractionation on an isotope timeseries is illustrated in Figure S2. One advantage of the method by Bowen et al. (2018) is that it accounts for the uncertainty associated with the reconstructed source water. All the isotope profiles and timeseries shown in the paper refer to the source value, i.e., the value after the effect of isotope fractionation was removed.

To apply the method by Bowen et al. (2018), we need to estimate the "evaporation lines" (Gat, 1971), i.e., the trajectories of evaporative enrichment for ^{18}O and ^{2}H, and the LMWL of the experiment. Evaporation lines were computed through a standard implementation of the Craig-Gordon model (Benettin et al., 2018) for the range of temperature and humidity that characterized the period February to June 2018. The resulting evaporation lines have a slope of 3.2 ± 0.2 (mean ± standard deviation). The LMWL of the experiment was obtained by considering the isotopic composition of all the inputs to the lysimeter, weighted by their volume. These include: labeled tracer application, irrigation, and natural precipitation during the experiment, and the pre-existing soil water at the beginning of the experiment, which integrates the past unrecorded inputs to the lysimeter. This results in the equation: $\delta^2H = 8.26\delta^{18}O + 11.30$, which is in close agreement with the LMWL at other locations in the Lake Geneva area (e.g., Nyon, IAEA/WMO, 2020).

2.4. Computing Mass and Concentration Breakthrough Curves

Tracer breakthrough curves are a useful mean to quantify empirically the transport of a labeled input through a system. We computed normalized concentration and mass breakthrough curves (CBTC and MBTC, respectively) for bottom leakage, xylem water, and bulk soil water at the five available soil depths. The curves are normalized by the input mass to make them independent from the mass units. When computing tracer breakthroughs for water isotopes, one has to take into account that some tracer mass is always already present in the soil water before application of the labeled input and that additional tracer mass may be supplied through subsequent precipitation (see Section S2). Thus, we first computed a normalized isotope composition for each sample as:

$$\xi_k(t_i) = \frac{C_k(t_i) - C_{b_k}(t_i)}{(C_I(t_0) - C_0)V(t_0)} \tag{2}$$

where k denotes a sample type (e.g., bottom drainage or xylem water), t_i is the time when the sample was collected, t_0 is the time when the tracer was applied, $C_k(t_i)$ and $C_{b_k}(t_i)$ are the measured sample composition and the estimated isotopic composition contributed by waters other than the labeled irrigation (i.e., background concentration and contribution of subsequent rainfall or irrigation events), $V(t_0)$ is the labeled irrigation volume, $C_I(t_0)$ is the isotope composition of the labeled irrigation and C_0 is the average composition of water inputs to the lysimeter (excluding the labeled irrigation). The effect of Equation 2

is to separate for each sample the contribution of the labeled irrigation from other contributions and to normalize it to the input tracer mass. As such, it does not depend on mass units, as long as they are used consistently, and results in curves with units of volume^{-1} (in our case mm^{-1}). The terms $C_k(t_i)$ were characterized by the mean and standard deviation of the sample composition after the effect of isotope fractionation was removed. When duplicate samples were available on the same date (typically for bulk soil water, which was collected at two points at each depth), the average value and the standard deviation across samples (again, after fractionation was filtered out) were used to characterize $C_k(t_i)$. Thus, each data point $\xi(t_i)$ was characterized by a mean value and a standard deviation. For soil at 10 and 25 cm depth the CBTC was very pronounced in the first 10 days after tracer application and bulk soil samples collected every 4 days are insufficient to characterize it. Thus, for the first 10 days only, the isotope composition of soil water at 10 and 25 cm depth was obtained by combining both bulk soil samples and soil water samples from suction cups (that were collected every 2 days). As the lysimeter was rather wet in those first days, we expect minimal differences between bulk soil composition and soil water as sampled from suction cups. The background composition terms $C_{b_k}(t_i)$ were specific of each sample type, but in most cases, they were a simple linear interpolation between the composition before the tracer application and the composition after the breakthrough was over. Extensive details about the computation of the terms $\xi(t_i)$ are in Section S2.

Empirical CBTCs were computed from the normalized data $\xi(t_i)$ through simple linear interpolation. We also computed analytical CBTC by fitting the data points $\xi(t_i)$ with probability distribution functions (pdfs). For the deeper (50, 80, and 150 cm) bulk soil and bottom drainage samples we used inverse Gaussian distributions, which naturally result from tracer breakthrough in uniform, one-dimensional, steady-state advection dispersion models. For shallow (10, 25 cm) soil samples and xylem samples we used a Weibull distribution. The reason for shallow soil samples were fitted through a Weibull distribution is that the inverse Gaussian is not a good model for a finite spatial domain when dispersion is relatively strong (low Péclet numbers), and low Péclet numbers are usually expected in shallow soils.

For mass recovery computations and transit time distributions we computed MBTCs in all lysimeter outflows (i.e., bottom leakage, evaporation, and transpiration) by multiplying the relevant CBTCs by their corresponding water fluxes. Given that we did not measure the water vapor leaving the soil column, we assumed that the tracer breakthrough in the evaporation flux reflected the breakthrough of bulk soil water at 10 cm (which comprised soil between 6 and 10 cm depth). The residual tracer mass that was still within the soil column at the end of the experiment was estimated from the three different soil cores taken during the final destructive sampling (cores of 8 cm diameter, sampled by vertical increments of 10 cm down to a depth of 200 cm). We applied a formula equivalent to Equation 2 over space to obtain an average tracer concentration profile across the three cores and multiplied by soil moisture and integrated across the profile to get the total residual tracer mass. The balance closure error, normalized to the mass input, is quantified through the equation:

$$\epsilon = 1 - \Phi_R - \Phi_L - \Phi_T - \Phi_E \tag{3}$$

where ϵ is the mass imbalance, the terms Φ are total tracer mass at the different outlets, and subscripts R, L, E, T refer to residual mass, bottom leakage, evaporation, and transpiration, respectively. Being normalized by the mass input, all terms of Equation 3 are non-dimensional and range within 0–1.

3. Results

3.1. Hydrologic Data

Hydrologic data measured from the beginning to the end of the experiment is shown in Figure 2. From 10 May 2018 to 1 July 2018, the lysimeter received input water from rainfall (199 mm) and irrigation (489 mm) and released 613 mm of water by evapotranspiration and 83 mm by bottom drainage. The irrigation additions toward the end of the experiment brought the lysimeter from dry to wet conditions, such that the net storage variations between the experiment start and end were almost null (−9 mm). Bottom flow and moisture data (panels b and d) show that the experiment underwent 4 main wetting-drying cycles. Tracer application took place during wet conditions but the high ET rates quickly turned the column to dry conditions

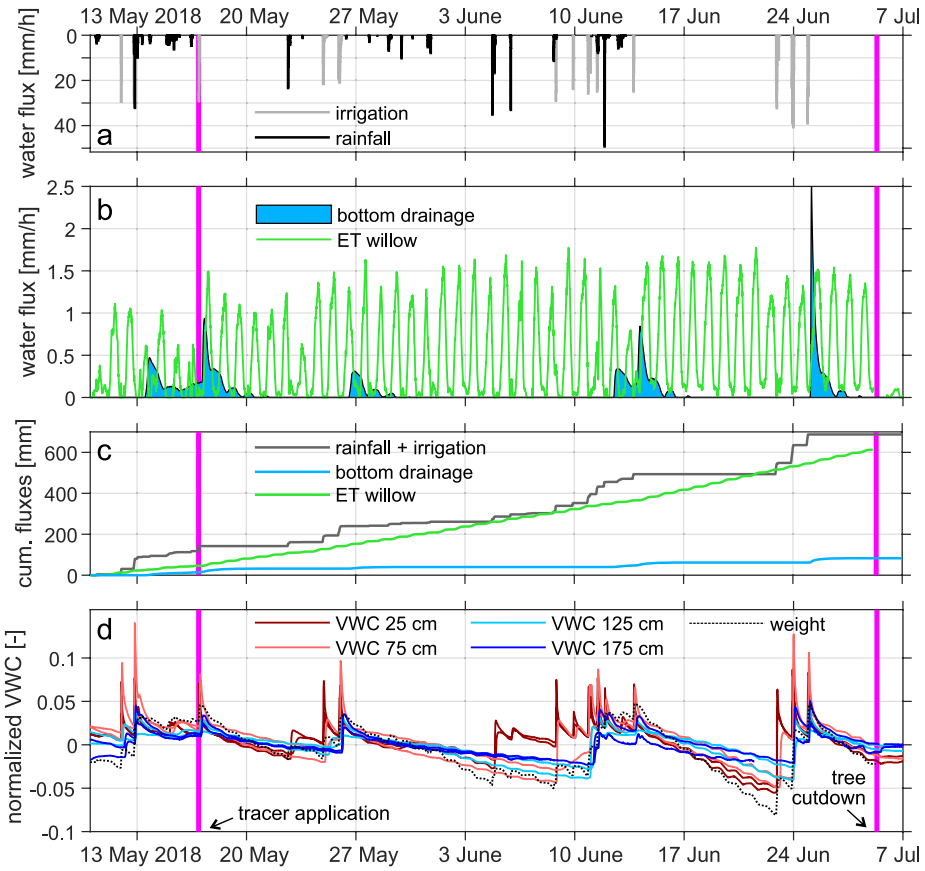

Figure 2. Timeseries of input/output fluxes to the lysimeter (a–c) and weight and moisture at various depths normalized by their mean and standard deviation (d). Vertical bars indicate the beginning and the end of the experiment. The hydrologic conditions during the 43 experiment days were characterized by mostly low to null bottom drainage flow, high ET rates, and a sequence of four major wet-dry cycles.

with zero drainage after 4 days. Successive rainfall and irrigation increased the volumetric water content, but rewetting was very variable and often the new water inputs did not prompt any reaction to volumetric water content at 75 cm depth or lower (see e.g., the week between 3 June and 10 June). Even when bottom flow was reactivated, it usually ceased after 3 days and, overall, bottom flow was only observed 30% of the time. The driest conditions were reached in the period 17–20 June, after 10 days without any water input and a cumulative loss of 140 mm of water to ET.

The diurnal ET cycles typically started at 6 a.m., peaked at 2–4 p.m., and ended at 8 p.m.. Daily ET increased from 10 mm/d in early May to 18 mm/d in late June, with an average of 13 mm/d. These ET rates are high but consistent with previous experiments on the same genetic species (Gorla et al., 2015; Queloz et al., 2015) and fully in agreement with values for the genus *Salix* at high density (1.79 plants per m^2) in controlled field conditions (Frédette et al., 2019). Although irrigation was provided to the willow-planted lysimeter only, ET patterns are generally consistent across the four lysimeters (Figure 3). ET rates in the grass-planted lysimeters (red and orange curves in Figure 3) were on average 5 mm/d (less than half as in the willow-planted lysimeter) and evaporation from bare soil (purple curves) was roughly 2 mm/d. The day after the willow was cut, ET in the willow-planted lysimeter dropped to a value of 1 mm/d.

3.2. Soil Isotope Profiles

The evolution of the isotopic profile of the soil column is shown for $\delta^{18}O$ in Figure 4. Isotope compositions are represented through errobars that indicate the mean and the standard deviation across measurements at the same depth. Before tracer application (panel A), the profile is rather uniform around the value of

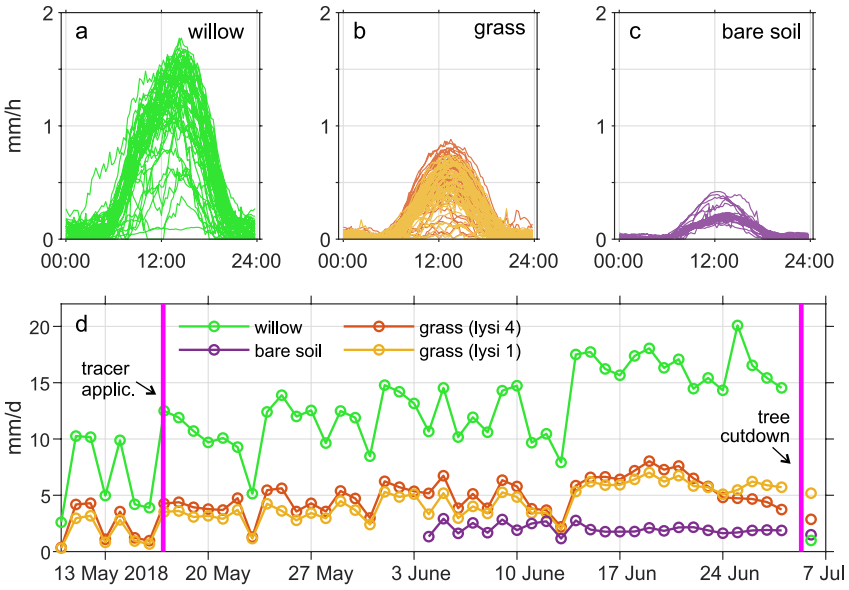

Figure 3. Evapotranspiration computed from weight variations at all four lysimeters: hourly patterns (a, b, c in mm/h) and daily patterns (d, in mm/d). ET flux at the willow lysimeter (green color) ranged between 5 and 20 mm/d and it dropped to 1 mm/d (less than ET flux from bare soil lysimeter) after the tree was cut down.

−11‰, which reflects winter precipitation in the surrounding lake Geneva area and tap water additions, but the top of the soil column was more enriched due to natural heavier precipitation that occurred right before the experiment start. In the first week after tracer application (panel B), the tracer remained confined at the top of the lysimeter (with $\delta^{18}O$ getting as high as +17‰). Although there was strong spatial heterogeneity (which results in larger error bars) the mean profile was consistent whether it was evaluated through soil water (from suction cups) or bulk soil water samples. After two weeks since tracer application (panel C) the tracer front moved down to the depth of 50 cm, while the top of the lysimeter returned back to

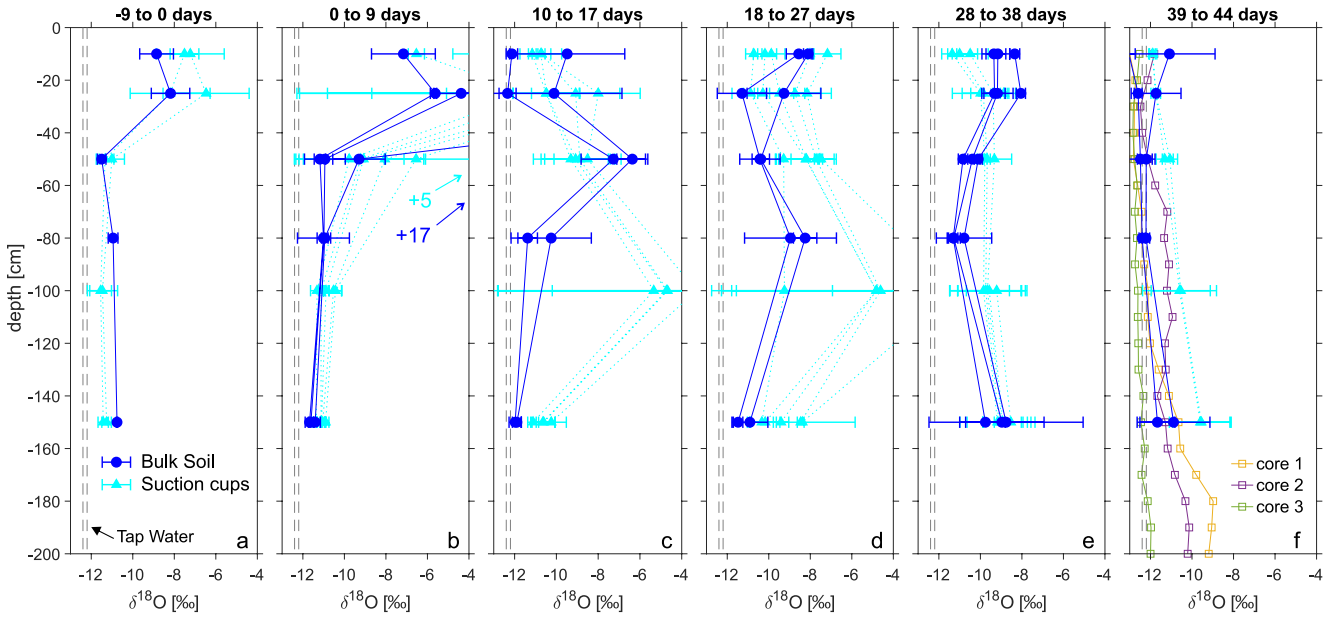

Figure 4. Evolution of the soil isotopic profile during the experiment. Blue indicates bulk soil samples and cyan indicates soil water sampled from suction cups. Error bars indicate the mean and standard deviation across replicas at the same depth. Vertical lines indicate the reference isotope composition before the beginning of the experiment (which reflects winter rainfall and tap water irrigation). The last panel (f) also features the three soil cores taken at the end of the experiment.

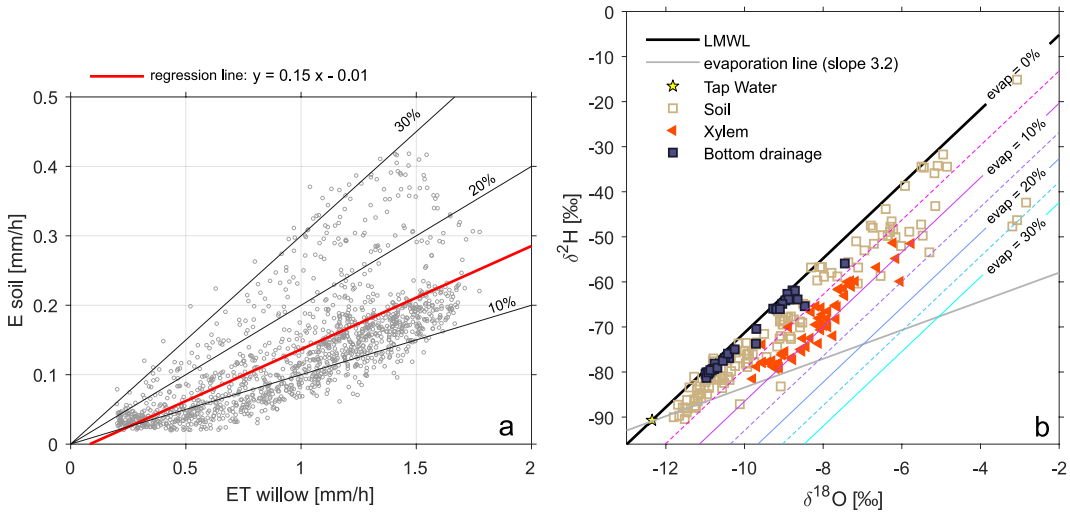

Figure 5. Relationship between evaporation in the bare soil lysimeter and evapotranspiration in the willow lysimeter. The ratio E/ET is on average 15%, but evaporation in the willow lysimeter is expected to be lower due to the presence of the willow tree (a). Dual isotope plot with evaporative fractions computed from the Craig-Gordon model. Most samples are compatible with 5%–10% evaporation (b).

pre-tracer-application level because of the new inputs (rain and irrigation) with lighter isotope composition. During this period, the front observed through soil water appeared to move faster as it reached the suction cups located at 100 cm. After the third week (panel D) the front reached the depth of 80 cm in the bulk soil and after 4 weeks (panel E) it reached the depth of 150 cm. The last plot (panel F) compares profiles taken at the end of the experiment through high-resolution soil cores with the profiles obtained from suction cups and bulk soil samples. Spatial heterogeneity is evident, but the profiles consistently show that a substantial portion of the tracer is still within the soil column, mostly located below 150 cm depth.

3.3. E/ET Partitioning

Hydrologic and isotope data may help us estimate the fraction of evaporation over the total evapotranspiration at the willow-planted lysimeter. First, we compared the evaporation rates computed at the bare soil lysimeter (E_s) against the evapotranspiration rates in the willow-planted lysimeter (ET_w). This relationship does not provide a direct estimate of E/ET because it comes from two different systems, but it provides a useful reference value. The relationship between E_s and ET_w (Figure 5a) is rather variable over the days (E_s/ET_w ranges in 5%–30%) with an average E_s/ET_w ratio of 15%. Evaporation from the bare soil is expected to be generally higher than evaporation from the willow-planted lysimeter because the presence of the willow limits soil evaporation (due to the physical space occupied by the willow, shading, root water uptake). This also becomes clear by noting that, after the willow plants were cut, ET_w rates dropped to values that were lower than E_s (Figure 3b, last day). Additionally, we used the Craig-Gordon model to estimate the isotope composition of samples subject to different fractions of evaporation (Figure 5b). In dual-isotope space, these evaporation fractions take the form of lines parallel to the LMWL and progressively shifted rightwards. The majority of samples are compatible with 5%–10% E/ET ratios. Thus, by combining hydrologic data with isotope information, the E/ET ratio is assumed to be 10% on average.

3.4. Tracer Breakthrough Curves

The normalized concentration breakthrough curves, computed according to Section 2.4, are shown in Figure 6. The breakthrough in the transpiration flux (obtained from xylem water samples) started and peaked immediately after tracer application and then slowly decreased with irregular oscillations until the end of the experiment, when the breakthrough was not entirely over. The tracer breakthrough in the lysimeter drainage was discontinuous due to frequent absence of bottom flow. Its behavior was somewhat opposite to that of transpiration in that the tracer was mainly released after 25 days and the breakthrough was not en-

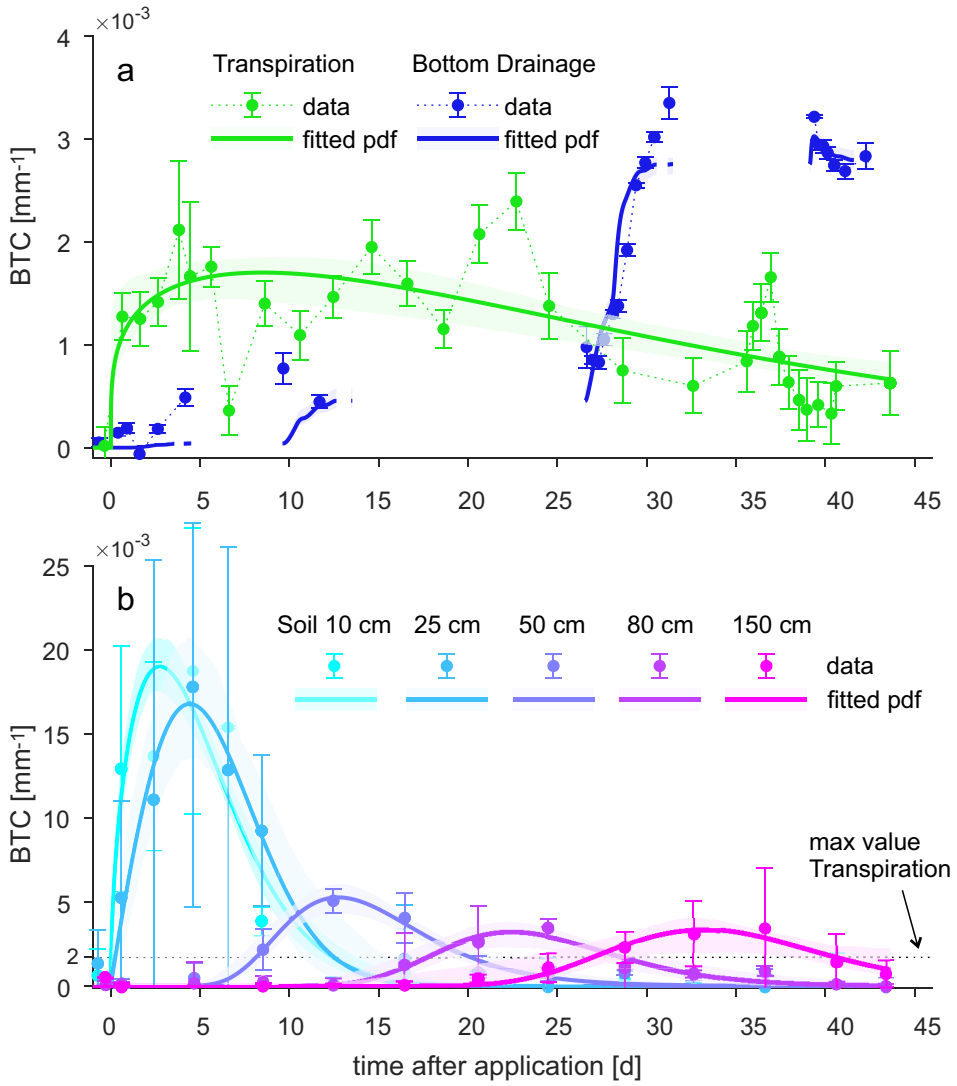

Figure 6. Tracer breakthrough curves for bottom drainage and transpiration (a) and for soil at different depths (b). Soil samples come from bulk soil sampling except for 10 and 25 cm where it is an average of both bulk soil and mobile water samples (see Section 2.4). Dots with error bars represent data and the solid line is the fitting pdf with confidence intervals. The BTC of bottom drainage is discontinuous because of periods of no flow. Note that plot b has a different scaling to accommodate the pronounced breakthrough in the top soil and a dotted line indicates the maximum value of the transpiration BTC as a reference.

tirely over at the end of the experiment. The breakthrough in the soil column (Figure 6b) reflects the timing at which the tracer reached the different depths. The top of the lysimeter (10 and 25 cm) had a very pronounced early breakthrough characterized by large spatial heterogeneity (large error bars in the plot). The breakthrough at lower depths (50, 80, and 150 cm) was much more damped and regular. The effect of preferential flow is evident as, similar to Benettin et al. (2019), the peak in the bottom drainage occurs at the same time as the peak in the soil at 150 cm. Note that the plots have different scaling and that the transpiration BTC remains very low (max 2×10^{-3} mm^{-1}) compared to the BTC in the topsoil (max 20×10^{-3} mm^{-1}). The smooth pdfs and the simple linear interpolation of the normalized data generally match, except in the case of transpiration BTC where the general trend is well matched by the pdf but not the irregular oscillations.

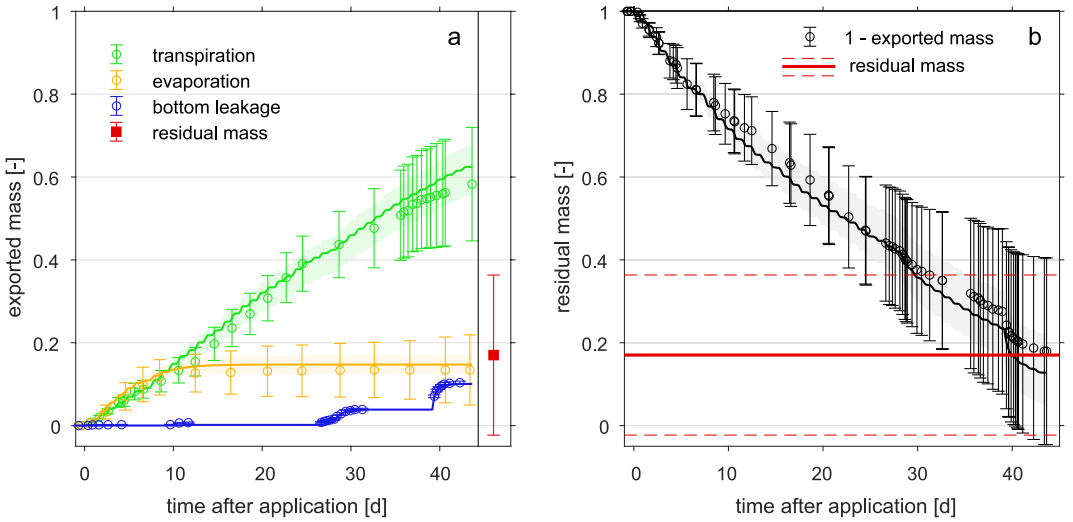

Figure 7. Cumulative tracer mass exported from each hydrologic flux (a) and residual mass throughout the experiment (b). Data is indicated by error bars. Solid lines with shaded confidence intervals indicate the fitted pdf as in Figure 6. The residual mass estimated from the three soil cores is indicated in red in both plots. Although the heterogeneity of the system results in broad uncertainty bands, the average curve shows a good balance closure.

4. Discussion

The work presented here is a direct response to recent calls by Soulsby et al. (2016) for characterizing the age distribution of catchment evaporative losses, something largely still beyond our reach in the field. So too the recommendations in Sprenger et al. (2019) who advocated "to further develop sampling designs and new measurement techniques" and "better understanding of where, when, and how often to take samples in tracer hydrological investigations" for improving our understanding of the demographics of water in the critical zone. Below we return to our research questions and reflect on our findings and their connection to the broader work linked to mechanistic assessment of the water balance.

4.1. Closing the Water Balance; Tracing the Water Balance

Our nearly complete mapping of the hydrologic fluxes (Figures 2 and 3) and tracer compositions (Figures 4–6) allows us to test the tracer mass balance closure (Equation 3). From a purely-hydrometric perspective, the water storage at the end of the experiment almost returned to its initial value before the beginning of experiment, and 680 mm of water transited the soil column. The outflow was largely dominated by evaporation and transpiration fluxes (88%), mainly due to the high transpiration rates of the willow tree. While weighed lysimeters allow great precision in the determination of water balance components (Groh et al., 2020), most field investigations rely on less sophisticated systems. Even more problematic would be the direct determination of ET fluxes through models. For these reasons, the water balance remains "unclosed" at many locations and a precise quantitative result measured here may be a guide to extend, say to large and diverse assemblages of vegetation, features that prove relevant in this context. In any case, even a perfect hydrometric balance closure provides the average precipitation partitioning during the entire experiment, but this an "apparent" closure that does not distinguish water that entered the lysimeter through precipitation and its loss or use before the end of the experiment. This underscores the black box nature of the water balance accounting model where the average partitioning can be very different from the partitioning of individual rainfall events. So how does the tracer-based view of the water balance compare to the traditional hydrometric closure? Like the simple hydrometric calculation, the exported mass (Figure 7a) is dominated by the transpiration fluxes (58%), with minor contributions from soil evaporation (13.4%) and bottom drainage (10.4%). The overall mass that left the soil column in the 43 days after the application (82%, see Figure 7b) agrees well with the residual mass that was determined independently through the soil core analysis at the end of the experiment (17%). This leaves a very small imbalance (1%) and shows that, despite the uncertainty, the mass balance of the labeled irrigation is almost perfectly closed. But beyond closure, the

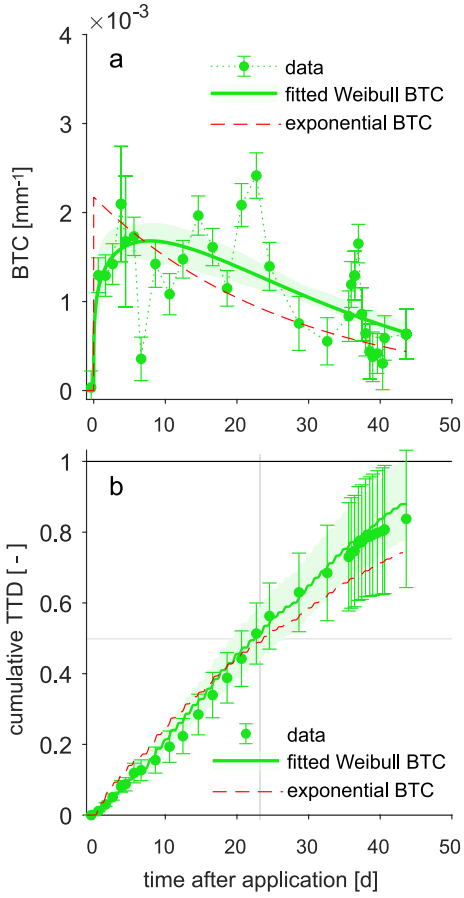

Figure 8. Concentration breakthrough curve (a) and cumulative travel time distribution (b) for the transpiration flux as inferred from: xylem sample data (green errorbars), Weibull pdf fitted to the data (green solid line with confidence intervals), Exponential pdf with parameter k equal to the ratio between the mean lysimeter storage and mean transpiration during the experiment (red dashed line). The median travel time is indicated by gray lines. The data reveals an irregular breakthrough in the transpiration flux, but the trend is generally matched by the fitted Weibull pdf. The Exponential pdf is the ideal behavior that would be expected in a randomly-sampled system.

tracer provides an illumination of the traditional black box water balance accounting. Our tracing of the rain event allowed us to trace the transpiration flux and determine the age of the transpired water relative to soil water and bottom drainage fluxes.

4.2. The Age of the Transpiration Flux

The value of the tracer-based water balance analysis is its ability to characterize the age of the water balance components. For instance, the concentration breakthrough curves (Figure 6) reveal the relative timing at which the tracer was found in different parts of the lysimeter system. As expected in our 1D column system, the tracer is progressively dispersed as infiltrating water moves to lower depths. The bottom drainage breakthrough had a clear peak that, despite the presence of preferential flow, only started 30 days since tracer application. Contrasting with this behavior, the tracer breakthrough of the transpiration flux was very flat and damped throughout the experiment. The tree immediately accessed the labeled irrigation. But, the total tracer water use in the top 25 cm of the lysimeter (e.g., days 0–10) was only a small component of soil water uptake. The prolonged transpiration breakthrough suggests that there was no characteristic uptake depth and that the plant, on average, used water from all depths. The tracer breakthrough (Figure 6a) also had irregular fluctuations that likely reflected some progressive shift toward shallower/deeper sources depending on tree water status as outlined in Nehemy et al. (2021). This behavior is consistent with the observed root architecture: fine roots (<2 mm) were observed throughout the entire soil column, up to 2 m depth (Nehemy et al., 2021). The relative uniform and deep presence of fine roots suggests that water uptake was not constrained to any depth or sector.

The residence times of rainfall to transpiration can be inferred from the MBTC (Figure 7a) after normalizing by the tracer recovery in the transpiration flux, which is expected to be 70% in this case. The resulting travel time distribution (Figure 8) indicates that the first 10% of labeled irrigation reached the plant within 5 days and the first 50% (i.e., the median of the distribution) in 22 days. We could not compute the travel time distribution after 43 days because the experiment ended, but even with a longer experiment the right-tail of the distribution would have been difficult to estimate because the tracer was close to background levels. The observed breakthrough was also similar to an exponential distribution, with parameter k obtained from the ratio between the mean transpiration flux and the mean storage during the experiment ($k = 27.2$ days). The exponential pdf emerges automatically in steady-state systems when a tracer is either well-mixed within the storage or when it is randomly-sampled (Benettin et al., 2013; Botter et al., 2010) by the outflow. Like the data itself, the Weibull pdf and the exponential pdf are broadly comparable for this tracer breakthrough (Figure 8) and they are markedly different from any other breakthrough curve measured in the lysimeter. The tracer profiles (Figure 4) show that the tracer is far from being well mixed in this experiment. Therefore, we hypothesize that the root architecture acts as a random sampler where, on average, the different water parcels are taken up proportionally to their abundance. This behavior, which is favored by root water uptake compensation mechanisms (Cowan, 1965; De Jong Van Lier et al., 2006) suggests that a random sampling may occur without invoking a complete mixing of the tracer within the soil.

4.3. How is Knowing the Age of the Transpiration Flux Useful?

Water age has no influence on root water uptake. However, the age of transpiration reflects the coupling between the distribution of water ages that are available within the soil, the plant-specific access to those waters, and the tree hydraulic traits that affects the transport velocity (Gaines et al., 2016; Steppe et al., 2006). Quantifying the age of transpiration helps us go beyond the traditional hydrometric accounting model and to understand *which* water is available to plants; and which precipitation events or seasons sustain most the plant water needs (Allen et al., 2019). For the willows in our experiment, about 60% of the tracer that was routed to the plant was transpired within a month. The intense water inputs and high transpiration rates resulted in short turnover times and under these conditions the plant appeared to be sustained by precipitation that entered the lysimeter during the previous 1–2 months. Our results contrast with the labeled-irrigation experiment by Evaristo et al. (2019) who studied the age of transpired water in the Biosphere 2 tropical ecosystem. The Evaristo et al. (2019) work is the only other study that we are aware of that has reported the BTC in the transpiration flux. In that experiment, which was conducted after a prolonged drought, water moved quickly through the soil profile (mean time to leakage was about 9 days) and the water transpired by trees was consistently 2–7 times older than this leakage. Instead, in our much smaller system we found that rainfall reached the willow faster than it reached the bottom of the column. Of course our experiment was conducted in a different soil and climate, on a different tree species, and under different wetness conditions. We hypothesize that the lack of drought stress in our system, tree size, and hydraulic characteristics contributed to earlier BTC than the ones observed by Evaristo et al. (2019). Salix spp. are known by high transpiration rates (Frédette et al., 2019) and high wood density ($\rho = 0.55$ g/cm^3), thus low sapwood capacitance (Oliva Carrasco et al., 2015; Scholz et al., 2007). The high wood density and low sapwood capacitance indicates small use sapwood storage to daily transpiration, but ability to withstanding quite negative xylem water potentials, and maintain high velocities (Mcculloh et al., 2012; Meinzer et al., 2009). Even with similar sapwood hydraulic characteristics to the species with faster BTC, our S. viminalis is almost 10 times shorter in height than individuals at Biosphere 2, thus the tracer traveled much shorter distances before reaching the canopy. Thus, it is perhaps not surprising that these results are so different. Yet, both works reveal the importance of tracing the water balance and revealing the hitherto unexplored complexity of transpiration versus groundwater recharge (i.e., bottom drainage in the lysimeter) processes and mechanistic assessment of the main fluxes.

4.4. Uncertainty in Water Balance Apportionment

We made several assumptions in this work. The isotope composition of the evaporation flux was assumed to be equal to that of soil water measured at 6–10 cm depth (besides fractionation effects, which were removed). While this may not be true for short-term evaporation dynamics, we expected this approximation to hold on average over the duration of the experiment. We assumed that plant water storage was negligible and that the composition that we measured in the stems' xylem water was equivalent to the composition taken up by the roots. Knighton et al. (2020) showed that for small trees with high transpiration rates, as in our case, this is a reasonable assumption. We also assumed implicitly that water taken up by vegetation was removed permanently from the soil. This may not have been completely realistic if plant water hydraulic redistribution occurred (Caldwell et al., 1998; Dawson, 1993; Neumann & Cardon, 2012). Thus we did not consider the possible occurrence of hydraulic redistribution nor the possibility that root exudates might affect the mobility of water close to the root surface. Whether or not this is quantitatively important for the water balance will probably depend on case-specific circumstances (Dawson, 1993).

Uncertainty in our tracer breakthrough estimates comes from two main factors: 1) since transpiration was by far the main water balance outflow, the relatively small uncertainties in the xylem isotope composition, related to the necessary removal of evaporative fractionation effects, may be enhanced compared to the uncertainty in the other samples; and 2) the soil showed strong spatial heterogeneity in the isotope composition (e.g., at the end of the experiment one soil core had almost no residual tracer while the other two cores had substantial amounts, see Figure 4f), and this led to large uncertainty bounds. With these results, we deduce that a lower uncertainty is expected when the xylem samples are less fractionated or when the main outflow is the bottom drainage (as expected in the winter time), which is typically less fractionated (Evaristo et al., 2015). The spatial variability in the soil samples is a well-known problem that is

difficult to resolve without increasing the sampling effort. Our results may have been less uncertain if the isotopic profile at the beginning of the experiment had been more uniform and the natural rainfall –with its strong temporal variability in isotope composition– prevented as in Queloz et al. (2015). However, this would have required sheltering the lysimeter surface and compensating rainfall with real-time irrigation (see Pangle et al., 2014). In the trade-off between the degree of realism and manipulation, the need for more accurate results may necessitate increased manipulation at the cost of making the experiment more artificial. In terms of tracers, a different choice (e.g., bromide) would have avoided the environmental variability of the water stable isotopes (which affects the terms C_{b_k} and C_0 in Equation 2 and generally makes it easier to measure the tail of the BTC), but it would have prevented the direct estimate of the water mass that exits through transpiration, which was our main focus here. Finally, we note that accurate measurements of all the water fluxes are necessary to achieve a good tracer balance closure, but in field conditions these fluxes may not be easy to determine. For example, the tipping bucket next to the lysimeter field recorded a precipitation that was 5%–7% lower than measured in the lysimeters; the ET modeled using an uncalibrated Penman-Monteith equation, besides neglecting nighttime ET, would have provided a roughly 10% lower estimate; the E/ET partitioning, even in the presence of lysimeter and isotope measurements, was uncertain and is typically challenging and ecosystem dependent (Stoy et al., 2019). This highlights how difficult it can be even a conceptually simple task like closing the hydrometric and tracer balance–experimentally.

4.5. Needed Next Steps

Our experimental mass balance closure coupled with the tracing of water balance components and calculation of the ages of all the fluxes is perhaps an example for what might be attempted next. Notwithstanding, our work is for just one single labeled "event." Complete experimental closure for a higher number of precipitation events is needed. This will be difficult because, unless one sticks to a periodic water and tracer application (Harman & Kim, 2014), each rain input should be labeled by a different, detectable tracer, which in turn can be likewise measurable for each and every outflow. Such an approach, while much needed, is currently infeasible. The Lagrangian mass balance closure that we have presented is only possible for an experimental setting like a large lysimeter or for extra-ordinary infrastructure like the Landscape Evolution Observatory (Volkmann et al., 2018). So whilst tracer experiments at the scale of an entire catchment still appear infeasible, smaller-scale experiments of the kind we have presented can help address key ecohydrologic questions and base for theoretically sound upscaling from local evidence to catchment and basin scales. A natural extension of this work would be a series of tracer experiments in the field to evaluate the time at which different plants in the same natural environment uptake one or more labeled irrigations. The use of new in situ technology to measure the isotope composition of xylem water is promising (Beyer et al., 2020) and may allow high-resolution monitoring over prolonged periods. Closing the tracer balance in the field would be challenging because of the difficulties in sampling subsurface fluxes, but hypotheses about the temporal origin of plant transpiration could be tested.

The approach recommended here may help investigate how landscape ecohydrological properties change with altered precipitation regimes. Soil and plant ecological characteristics, including the makeup of soil microbial communities (Delgado-Baquerizo et al., 2018; Magnabosco, 2018) that are known to be affected by hydrologic fluctuations, change with altered precipitation regimes. Addressing the related effects on ecosystem processes and functions in such work will enhance the value of experiments of this kind. This holds, in particular, if one is specifically interested in testing how changes in precipitation may possibly lead to crossing of biological thresholds affecting ecosystem resilience, and ultimately transport at the catchment scale.

5. Conclusions

Our work has presented empirical evidence for water balance closure and tracing for a vegetated lysimeter. We leveraged high-resolution hydrometric and tracer data to quantify the tracer breakthrough curves in all water fluxes including transpiration. Plant uptake was by far (58%) the largest conduit for labeled irrigation water removal, while only a small amount (10%) left as bottom drainage during the 43 days of tracing.

The water balance fluxes were also characterized by substantially different tracer breakthrough curves and travel times. While the delayed tracer breakthrough in the bottom drainage reflected the interplay between matrix and preferential flow through the soil, the damped breakthrough in the transpiration flux reflected the rather uniform root architecture of the willow tree. Under our experimental conditions, the willow tree relied on waters that infiltrated into the soil in the previous 1–2 months. This work shows how tracing the water balance fluxes can illuminate the black box of the traditional hydrometric water balance closure approach.

Data Availability Statement

All data presented in this paper is available at http://doi.org/10.5281/zenodo.4037240 (Nehemy et al., 2020), under Creative Commons Attribution (CC BY) license.

Acknowledgments
A. Rinaldo and P. Benettin thank ENAC school at EPFL for financial support and acknowledge the Swiss National Science Foundation grant number CRSII5_186422. We thank the ECHO lab crew, Pierre Queloz, and Scott Allen for precious help during the experiment, Gabriel Cotte and Torsten Vennemann from University of Lausanne (CH) for the collection and analysis of atmospheric vapor samples, James Kirchner for insightful comments. We thank Dr. Florian Heinlein and Dr. Janis Groh for their comments.

References

Ala-aho, P., Tetzlaff, D., McNamara, J. P., Laudon, H., & Soulsby, C. (2017). Using isotopes to constrain water flux and age estimates in snow-influenced catchments using the STARR (spatially distributed tracer-aided rainfall-runoff) model. *Hydrology and Earth System Sciences*, *21*(10), 5089–5110. https://doi.org/10.5194/hess-21-5089-2017

Allen, S. T., Kirchner, J. W., Braun, S., Siegwolf, R. T. W., & Goldsmith, G. R. (2019). Seasonal origins of soil water used by trees. *Hydrology and Earth System Sciences*, *23*(2), 1199–1210. https://doi.org/10.5194/hess-23-1199-2019

Asadollahi, M., Stumpp, C., Rinaldo, A., & Benettin, P. (2020). Transport and water age dynamics in soils: A comparative study of spatially integrated and spatially explicit models. *Water Resources Research*, *56*(3). https://doi.org/10.1029/2019wr025539

Benettin, P., Nehemy, M. F., Cernusak, L. A., Kahmen, A., & McDonnell, J. J. (2021). On the use of leaf water to determine plant water source: A proof of concept. *Hydrological Processes*, e14073. (in press) https://doi.org/10.1002/hyp.14073

Benettin, P., Queloz, P., Bensimon, M., McDonnell, J. J., & Rinaldo, A. (2019). Velocities, residence times, tracer breakthroughs in a vegetated lysimeter: A multitracer experiment. *Water Resources Research*, *55*(1), 21–33. https://doi.org/10.1029/2018wr023894

Benettin, P., van der Velde, Y., van der Zee, S. E. A. T. M., Rinaldo, A., & Botter, G. (2013). Chloride circulation in a lowland catchment and the formulation of transport by travel time distributions. *Water Resources Research*, *49*(8), 4619–4632. https://doi.org/10.1002/wrcr.20309

Benettin, P., Volkmann, T. H. M., von Freyberg, J., Frentress, J., Penna, D., Dawson, T. E., & Kirchner, J. W. (2018). Effects of climatic seasonality on the isotopic composition of evaporating soil waters. *Hydrology and Earth System Sciences*, *22*(5), 2881–2890. https://doi.org/10.5194/hess-22-2881-2018

Berghuijs, W. R., & Kirchner, J. W. (2017). The relationship between contrasting ages of groundwater and streamflow. *Geophysical Research Letters*, *44*(17), 8925–8935. https://doi.org/10.1002/2017GL074962

Beyer, M., Kühnhammer, K., & Dubbert, M. (2020). In situ measurements of soil and plant water isotopes: A review of approaches, practical considerations and a vision for the future. *Hydrology and Earth System Sciences*, *24*(9), 4413–4440. https://doi.org/10.5194/hess-24-4413-2020

Botter, G., Bertuzzo, E., & Rinaldo, A. (2010). Transport in the hydrologic response: Travel time distributions, soil moisture dynamics, and the old water paradox. *Water Resources Research*, *46*. https://doi.org/10.1029/2009WR008371

Bowen, G. J., Putman, A., Brooks, J. R., Bowling, D. R., Oerter, E. J., & Good, S. P. (2018). Inferring the source of evaporated waters using stable h and o isotopes. *Oecologia*, *187*(4), 1025–1039.01. https://doi.org/10.1007/s00442-018-4192-5

Brooks, J. R., Barnard, H. R., Coulombe, R., & McDonnell, J. J. (2010). Ecohydrologic separation of water between trees and streams in a Mediterranean climate [Journal Article]. *Nature Geoscience*, *3*(2), 100–104. https://doi.org/10.1038/ngeo722

Caldwell, M. M., Dawson, T. E., & Richards, J. H. (1998). Hydraulic lift: Consequences of water efflux from the roots of plants. *Oecologia*, *113*, 151–161. https://doi.org/10.1007/s004420050363

Cowan, I. R. (1965). Transport of water in the soil-plant-atmosphere system. *The Journal of Applied Ecology*, *2*(1), 221–239. https://doi.org/10.2307/2401706

Dawson, T. E. (1993). Hydraulic lift and water use by plants: Implications for water balance, performance and plant-plant interactions. *Oecologia*, *95*, 565–574. https://doi.org/10.1007/bf00317442

Delgado-Baquerizo, M., Oliverio, A. M., Brewer, T. E., Benavent-González, A., Eldridge, D. J., Bardgett, R. D., et al. (2018). A global atlas of the dominant bacteria found in soil. *Science*, *359*(6373), 320–325. https://doi.org/10.1126/science.aap9516

Evaristo, J., Jasechko, S., & McDonnell, J. J. (2015). Global separation of plant transpiration from groundwater and streamflow. *Nature*, *525*(7567), 91–94. https://doi.org/10.1038/nature14983

Evaristo, J., Kim, M., Haren, J., Pangle, L. A., Harman, C. J., Troch, P. A., & McDonnell, J. J. (2019). Characterizing the fluxes and age distribution of soil water, plant water, and deep percolation in a model tropical ecosystem. *Water Resources Research*, *55*(4), 3307–3327. https://doi.org/10.1029/2018wr023265

Frédette, C., Labrecque, M., Comeau, Y., & Brisson, J. (2019). Willows for environmental projects: A literature review of results on evapotranspiration rate and its driving factors across the genus salix. *Journal of Environmental Management*, *246*, 526–537. https://doi.org/10.1016/j.jenvman.2019.06.010

Freyberg, J., Allen, S. T., Grossiord, C., & Dawson, T. E. (2020). Plant and root-zone water isotopes are difficult to measure, explain, and predict: Some practical recommendations for determining plant water sources. *Methods in Ecology and Evolution*, *11*(11), 1352–1367. https://doi.org/10.1111/2041-210x.13461

Gaines, K. P., Meinzer, F. C., Duffy, C. J., Thomas, E. M., & Eissenstat, D. M. (2016). Rapid tree water transport and residence times in a pennsylvania catchment. *Ecohydrology*, *9*(8), 1554–1565. https://doi.org/10.1002/eco.1747

Gat, J. R. (1971). Comments on the stable isotope method in regional groundwater investigations. *Water Resources Research*, *7*(4), 980–993. https://doi.org/10.1029/WR007i004p00980

Gorla, L., Signarbieux, C., Turberg, P., Buttler, A., & Perona, P. (2015). Transient response of Salix cuttings to changing water level regimes. *Water Resources Research*, *51*(3), 1758–1774. https://doi.org/10.1002/2014WR015543

Groh, J., Stumpp, C., Lücke, A., Pütz, T., Vanderborght, J., & Vereecken, H. (2018). Inverse estimation of soil hydraulic and transport parameters of layered soils from water stable isotope and lysimeter data. *Vadose Zone Journal*, *17*(1), 170168. https://doi.org/10.2136/vzj2017.09.0168

Groh, J., Vanderborght, J., Pütz, T., Vogel, H.-J., Gründling, R., Rupp, H., et al. (2020). Responses of soil water storage and crop water use efficiency to changing climatic conditions: A lysimeter-based space-for-time approach. *Hydrology and Earth System Sciences*, *24*(3), 1211–1225. https://doi.org/10.5194/hess-24-1211-2020

Hannes, M., Wollschläger, U., Schrader, F., Durner, W., Gebler, S., Pütz, T., et al. (2015). A comprehensive filtering scheme for high-resolution estimation of the water balance components from high-precision lysimeters. *Hydrology and Earth System Sciences*, *19*(8), 3405–3418. https://doi.org/10.5194/hess-19-3405-2015

Harman, C. J., & Kim, M. (2014). An efficient tracer test for time-variable transit time distributions in periodic hydrodynamic systems. *Geophysical Research Letters*, *41*(5), 1567–1575. https://doi.org/10.1002/2013GL058980

IAEA/WMO. (2020). *Global network of isotopes in precipitation. the gnip database*. Retrieved from https://nucleus.iaea.org/wiser

Jasechko, S., Perrone, D., Befus, K. M., Bayani Cardenas, M., Ferguson, G., Gleeson, T., et al. (2017). Global aquifers dominated by fossil groundwaters but wells vulnerable to modern contamination. *Nature Geoscience*, *10*(6), 425–429. https://doi.org/10.1038/ngeo2943

Knighton, J., Kuppel, S., Smith, A., Soulsby, C., Sprenger, M., & Tetzlaff, D. (2020). Using isotopes to incorporate tree water storage and mixing dynamics into a distributed ecohydrologic modeling framework. *Ecohydrology*, *13*(3). https://doi.org/10.1002/eco.2201

Koeniger, P., Marshall, J. D., Link, T., & Mulch, A. (2011). An inexpensive, fast, and reliable method for vacuum extraction of soil and plant water for stable isotope analyses by mass spectrometry. *Rapid Communications in Mass Spectrometry*, *25*(20), 3041–3048. https://doi.org/10.1002/rcm.5198

Kuppel, S., Tetzlaff, D., Maneta, M. P., & Soulsby, C. (2018). EcH2O-iso 1.0: Water isotopes and age tracking in a process-based, distributed ecohydrological model. *Geoscientific Model Development*, *11*(7), 3045–3069. https://doi.org/10.5194/gmd-11-3045-2018

Magnabosco, C., Lin, L.-H., Dong, H., Bomberg, M., Ghiorse, W., Stan-Lotter, H., et al. (2018). The biomass and biodiversity of the continental subsurface. *Nature Geosciences*, *11*, 707. https://doi.org/10.1038/s41561-018-0221-6

Maxwell, R. M., Condon, L. E., Danesh-Yazdi, M., & Bearup, L. A. (2018). Exploring source water mixing and transient residence time distributions of outflow and evapotranspiration with an integrated hydrologic model and Lagrangian particle tracking approach. *Ecohydrology*, *12*, e2042, e2042. https://doi.org/10.1002/eco.2042

Mcculloh, K. A., Johnson, D. M., Meinzer, F. C., Voelker, S. L., Lachenbruch, B., & Domec, J.-c. (2012). Hydraulic architecture of two species differing in wood density: Opposing strategies in co-occurring tropical pioneer trees. *Plant, Cell and Environment*, *35*, 116–125. https://doi.org/10.1111/j.1365-3040.2011.02421.x

McDonnell, J. J. (2017). Beyond the water balance. *Nature Geoscience*, *10*(6), 396–396. https://doi.org/10.1038/ngeo2964

McGuire, K. J., & McDonnell, J. J. (2006). A review and evaluation of catchment transit time modeling. *Journal of Hydrology*, *330*(3–4), 543–563. https://doi.org/10.1016/j.jhydrol.2006.04.020

Meinzer, F. C., Johnson, D. M., Lachenbruch, B., Mcculloh, K. A., & Woodruff, D. R. (2009). Xylem hydraulic safety margins in woody plants: Coordination of stomatal control of xylem tension with hydraulic capacitance. *Functional Ecology*, *23*, 922–930. https://doi.org/10.1111/j.1365-2435.2009.01577.x

Nehemy, M. F., Benettin, P., Asadollahi, M., Pratt, D., Rinaldo, A., & McDonnell, J. J. (2020). Data set: The SPIKE II experiment - Tracing the water balance. *Zenodo*. https://doi.org/10.5281/zenodo.4037240

Nehemy, M. F., Benettin, P., Asadollahi, M., Pratt, D., Rinaldo, A., & McDonnell, J. J. (2021). Tree water deficit and dynamic source water partitioning. *Hydrological Processes*, *35*(1), e14004. https://doi.org/10.1002/hyp.14004

Neumann, R. B., & Cardon, Z. G. (2012). The magnitude of hydraulic redistribution by plant roots: A review and synthesis of empirical and modeling studies. *New Phytologist*, *194*, 337–352. https://doi.org/10.1111/j.1469-8137.2012.04088.x

Oliva Carrasco, L., Bucci, S. J., Di Francescantonio, D., Lezcano, O. A., Campanello, P. I., Scholz, F. G., et al. (2015). Water storage dynamics in the main stem of subtropical tree species differing in wood density, growth rate and life history traits. *Tree Physiology*, *35*(4), 354–365. https://doi.org/10.1093/treephys/tpu087

Pangle, L. A., Gregg, J. W., & McDonnell, J. J. (2014). Rainfall seasonality and an ecohydrological feedback offset the potential impact of climate warming on evapotranspiration and groundwater recharge. *Water Resources Research*, *50*(2), 1308–1321. https://doi.org/10.1002/2012WR013253

Pangle, L. A., Kim, M., Cardoso, C., Lora, M., Meira Neto, A. A., Volkmann, T. H. M., et al. (2017). The mechanistic basis for storage-dependent age distributions of water discharged from an experimental hillslope. *Water Resources Research*, *53*(4), 2733–2754. https://doi.org/10.1002/2016WR019901

Penna, D., Hopp, L., Scandellari, F., Allen, S. T., Benettin, P., Beyer, M., et al. (2018). Ideas and perspectives: Tracing terrestrial ecosystem water fluxes using hydrogen and oxygen stable isotopes - challenges and opportunities from an interdisciplinary perspective. *Biogeosciences*, *15*(21), 6399–6415. https://doi.org/10.5194/bg-15-6399-2018

Peters, A., Groh, J., Schrader, F., Durner, W., Vereecken, H., & Pütz, T. (2017). Toward an unbiased filter routine to determine precipitation and evapotranspiration from high precision lysimeter measurements. *Journal of Hydrology*, *549*, 731–740. https://doi.org/10.1016/j.jhydrol.2017.04.015

Queloz, P., Bertuzzo, E., Carraro, L., Botter, G., Miglietta, F., Rao, P. S. C., & Rinaldo, A. (2015). Transport of fluorobenzoate tracers in a vegetated hydrologic control volume: 1. experimental results. *Water Resources Research*, *51*(4), 2773–2792. https://doi.org/10.1002/2014WR016433

Rode, M., Wade, A. J., Cohen, M. J., Hensley, R. T., Bowes, M. J., Kirchner, J. W., et al. (2016). Sensors in the stream: The high-frequency wave of the present. *Environmental Science and Technology*, *50*(19), 10297–10307. https://doi.org/10.1021/acs.est.6b02155

Rodriguez-Iturbe, I. (2000). Ecohydrology: A hydrologic perspective of climate-soil-vegetation dynamies. *Water Resources Research*, *36*(1), 3–9. https://doi.org/10.1029/1999WR900210

Scholz, F. G., Bucci, S. J., Goldstein, G., Meinzer, F. C., Franco, A. C., & Miralles-wilhelm, F. (2007). Biophysical properties and functional significance of stem water storage tissues in Neotropical savanna trees. *Plant, Cell and Environment*, *30*, 236–248. https://doi.org/10.1111/j.1365-3040.2006.01623.x

Schrader, F., Durner, W., Fank, J., Gebler, S., Pütz, T., Hannes, M., & Wollschläger, U. (2013). Estimating precipitation and actual evapotranspiration from precision lysimeter measurements. *Procedia Environmental Sciences*, *19*, 543–552. https://doi.org/10.1016/j.proenv.2013.06.061

Soulsby, C., Birkel, C., & Tetzlaff, D. (2016). Characterizing the age distribution of catchment evaporative losses. *Hydrological Processes*, *30*(8), 1308–1312. (HYP-15-0908). https://doi.org/10.1002/hyp.10751

Sprenger, M., Stumpp, C., Weiler, M., Aeschbach, W., Allen, S. T., Benettin, P., et al. (2019). The demographics of water: A review of water ages in the critical zone. *Reviews of Geophysics*, *57*, 800. (in press). https://doi.org/10.1029/2018RG000633

Sprenger, M., Tetzlaff, D., Buttle, J., Laudon, H., & Soulsby, C. (2018). Water ages in the critical zone of long-term experimental sites in northern latitudes. *Hydrology and Earth System Sciences*, *22*(7), 3965–3981. https://doi.org/10.5194/hess-22-3965-2018

Steppe, K., De Pauw, D. J. W., Lemeur, R., & Vanrolleghem, P. A. (2006). A mathematical model linking tree sap flow dynamics to daily stem diameter fluctuations and radial stem growth. *Tree Physiology*, *26*(3), 257–273. https://doi.org/10.1093/treephys/26.3.257

Stoy, P. C., El-Madany, T. S., Fisher, J. B., Gentine, P., Gerken, T., Good, S. P., et al. (2019). Reviews and syntheses: Turning the challenges of partitioning ecosystem evaporation and transpiration into opportunities. *Biogeosciences*, *16*(19), 3747–3775. https://doi.org/10.5194/bg-16-3747-2019

van Lier, Q. d. J., Metselaar, K., & Van Dam, J. C. (2006). Root water extraction and limiting soil hydraulic conditions estimated by numerical simulation. *Vadose Zone Journal*, *5*, 1264–1277. https://doi.org/10.2136/vzj2006.0056

Volkmann, T. H. M., Haberer, K., Gessler, A., & Weiler, M. (2016). High-resolution isotope measurements resolve rapid ecohydrological dynamics at the soil-plant interface. *New Phytologist*, *210*(3), 839–849. https://doi.org/10.1111/nph.13868

Volkmann, T. H. M., Sengupta, A., Pangle, L. A., Dontsova, K., Barron-Gafford, G. A., Harman, C. J., et al. (2018). Controlled experiments of hillslope coevolution at the biosphere 2 landscape evolution observatory: Toward prediction of coupled hydrological, biogeochemical, and ecological change. In *Hydrology of artificial and controlled experiments*. InTech. https://doi.org/10.5772/intechopen.72325

von Freyberg, J., Studer, B., & Kirchner, J. W. (2017). A lab in the field: high-frequency analysis of water quality and stable isotopes in stream water and precipitation. *Hydrology and Earth System Sciences*, *21*(3), 1721–1739. https://doi.org/10.5194/hess-21-1721-2017

Wilusz, D. C., Harman, C. J., & Ball, W. P. (2017). Sensitivity of catchment transit times to rainfall variability under present and future climates. *Water Resources Research*, *53*(12), 10231–10256. https://doi.org/10.1002/2017wr020894

Yang, J., Heidbüchel, I., Musolff, A., Reinstorf, F., & Fleckenstein, J. H. (2018). Exploring the dynamics of transit times and subsurface mixing in a small agricultural catchment. *Water Resources Research*, *54*(3), 2317–2335. https://doi.org/10.1002/2017wr021896

Zhang, Z. Q., Evaristo, J., Li, Z., Si, B. C., & McDonnell, J. J. (2017). Tritium analysis shows apple trees may be transpiring water several decades old. *Hydrological Processes*, *31*(5), 1196–1201. https://doi.org/10.1002/hyp.11108